Journal of Medicinal Chemistry

Article

Bifunctional Chimera That Coordinately Targets Human Immunodeficiency Virus 1 (HIV-1) Envelope gp120 and Host Cell CCR5 Co-receptor at the Virus-Cell Interface

Adel A Rashad, Li-Rui Song, Andrew P Holmes, Kriti Acharya, Shiyu Zhang, Zhi-Long Wang, Ebony Gary, Xin Xie, Vanessa Pirrone, Michele A Kutzler, Ya-Qiu Long, and Irwin Chaiken

J. Med. Chem., **Just Accepted Manuscript** • DOI: 10.1021/acs.jmedchem.8b00477 • Publication Date (Web): 16 May 2018

ACS Publications

is published by the American Chemical Society. 1155 Sixteenth Street N.W., Washington, DC 20036

Bifunctional Chimera That Coordinately Targets Human Immunodeficiency Virus 1 (HIV-1) Envelope gp120 and Host Cell CCR5 Co-receptor at the Virus-Cell Interface

Adel A. Rashad[#1], Li-Rui Song[#2,3,4], Andrew P. Holmes[#1], Kriti Acharya[1], Shiyu Zhang[1,5], Zhi-Long Wang[2], Ebony Gary[6], Xin Xie[2], Vanessa Pirrone[7], Michele A. Kutzler[6], Ya-Qiu Long*[2,3], and Irwin Chaiken*[1]

[1] Department of Biochemistry and Molecular Biology, Drexel University College of Medicine, Philadelphia, PA 19102, USA; [2] CAS Key Laboratory of Receptor Research, Shanghai Institute of Materia Medica, Chinese Academy of Science, Shanghai 201203, China ; [3] College of Pharmaceutical Sciences, Soochow University Medical College, Suzhou 215123, China; [4] University of Chinese Academy of Sciences, No. 19A Yuquan Road, Beijing 100049, China; [5] School of Biomedical Engineering, Science and Health Systems, Drexel University, Philadelphia, PA 19104; [6] Department of Medicine, Drexel University College of Medicine, Philadelphia, PA 19102; and [7] Department of Microbiology and Immunology, Drexel University College of Medicine, Philadelphia, PA 19102, USA

[#] These authors contributed equally to this work.

ABSTRACT

To address the urgent need for new agents to reduce the global occurrence and spread of AIDS, we investigated the underlying hypothesis that antagonists of HIV-1 Envelope (Env) gp120 and host cell co-receptor (CoR) proteins can be covalently joined into bifunctional synergistic combinations that will improve antiviral. A synthetic protocol was established to covalently combine a CCR5 small molecule antagonist and a gp120 peptide triazole antagonist to form the bifunctional chimera. Importantly, the chimeric inhibitor preserved the specific targeting properties of the two separate chimera components, and at the same time exhibited low to sub-nanomolar potencies, in inhibiting cell infection by different pseudoviruses, that were substantially greater than those of a non-covalent mixture of individual components. The results demonstrate that targeting the virus-cell interface by a single molecule can result in improved potencies and also introduction of new phenotypes to the chimeric inhibitor such as irreversible inactivation of HIV-1.

INTRODUCTION

Inhibition of initial entry of HIV-1 into host cells remains a compelling yet elusive means to prevent infection and spread of the virus. HIV-1 cell infection is mediated by concerted interactions, at the virus-host cell interface, between trimeric envelope glycoprotein (Env) spikes on the virus membrane surface and two host cell receptors, CD4 and a co-receptor that is most commonly either CCR5 or CXCR4[1]. Each Env trimer consists of two non-covalently associated glycoproteins, a gp41 transmembrane protein and an external gp120 surface protein. During viral infection, CD4 interaction with the most exposed Env protein gp120 causes conformational rearrangement of the latter, leading to increased affinity co-receptor interaction at an initially cryptic site in gp120. This cascade exposes structural components in gp41 necessary to promote virus and cell membrane lipid mixing, fusion, pore formation, and infection. Inhibitors that can potently block virus-cell interactions and cell entry would hold great promise of inhibiting initial HIV-1 infection.

Currently approved inhibitors of entry steps are available clinically but have properties that limit their therapeutic usefulness. Maraviroc is an approved entry inhibitor that binds to the co-receptor CCR5 and prevents binding to HIV Env gp120 and, as a consequence, prevents full exposure of gp41 and suppresses virus-cell fusion[2, 3]. However, effectiveness of this drug requires matching the administered therapeutic to co-receptor use by the viral variants infecting each patient. In most cases, HIV infects cells after binding to the CCR5 receptor in the early stages of disease, but as the disease progresses, the virus can switch to another receptor, CXCR4. So, patients need to be tested for viral tropism before commencing CCR5 inhibition therapy. In addition, maraviroc induces tropism switch to CXCR4-expressing cells[4]. Hence, maraviroc is currently only approved for use in treatment-experienced patients[5]. Enfuvirtide (T20) is a 36-residue peptide that mimics part of the C-terminal helix in gp41 that mediates fusion. As such, it blocks binding of the gp41 N-terminal helix to C-

terminal helix and formation of the 6-helix bundle, which is the process that drives fusion between viral and cellular membranes. Due to its high cost of production, short drug half-life and the need for subcutaneous injections, enfuvirtide is also only approved as salvage therapy in patients who have failed multiple lines of therapy. Moreover, rapid mutations in a 10-residue stretch of gp41 N-terminal helix were observed to lead to resistance to this drug[6]. Recently, it also has been shown that HIV-1 can develop resistance to fusion inhibitors and become inhibitor-dependent, due to the critical kinetics required for these inhibitors[7].

Identifying new entry-targeting inhibitor approaches, in particular those that could function in combinations to increase potency and overcome viral resistance, remains an important goal of HIV-1 drug discovery efforts. To date, delineation of such combinations has been limited mainly to combinations of co-receptor inhibitors and T20[8-11]. Such combinations have demonstrated the potential for strong synergy with both CCR5 (TAK-220, SCH-C, and Aplaviroc) and CXCR4 (AMD-3100) inhibitors in assays of infection of peripheral blood mononuclear cells (PBMCs) with clinical HIV-1 isolates. Synergy between co-receptor inhibitors and Env gp41 inhibitor has been proposed to be due to kinetic linkage between the steps of entry that they antagonize[9-12]. This work points to the potential to achieve increased potency through combinations of inhibitors targeting different components of the virus-cell interface. This could be particularly important as new small-molecule co-receptor inhibitors are developed that target CXCR4 in addition to CCR5, as well as new inhibitors of the Env protein complex, including the most exposed protein component, gp120.

In the current work, we tested the hypothesis that covalent fusion of HIV-1 gp120 and co-receptor inhibitors could yield an HIV-1 cell infection inhibitor with enhanced potency compared to the sum of the potencies of the individual components. New classes of co-receptor inhibitors have been identified that can target either CCR5 or CXCR4 with strong antiviral effects[13-17]. At the same time, a class of gp120-targeting peptide triazoles (PTs) has

been identified that blocks both host cell receptor interactions and causes irreversible virus inactivation by triggering gp120 shedding[18, 19]. We chose LJC240[15] (co-receptor targeting, see **Figure 2** for structure) and UM15[20] (gp120-targeting, see **Figure 2** for structure) inhibitors for the initial prototype chimera components based on the already-established antiviral efficacies of these components on their own. The conjugation points of LJC240 to UM15 were determined by examining target-binding models as well as structure-activity relationships that identify structural elements, of the inhibitors, that are tolerant to modification. The protocol for the chimera synthesis was derived from the already-established solid phase synthesis of the peptide triazoles themselves[21-24] with follow-up sequential additions of linker and the free acid form of LJC240-COOH (**10**) before introducing the triazole by click conjugation. The functional properties of the resulting prototype chimera LJC240-L4-UM15 (**11**) were examined by a combination of cellular, virological and molecular assays. The results demonstrate that the covalent chimera retained individual component functions and at the same time a synergistically enhanced antiviral potency compared to a non-covalent mixture(s) of the 2 component inhibitors. The work provides strong support for the hypothesis that the bifunctional chimera could engage and synergistically block the infection-causing functions of host cell co-receptor and virus envelope gp120 at the HIV-1/cell interface.

RESULTS

1. Chimera Design and Synthesis

We designed a bifunctional molecule that is able to target both the HIV-1 envelope and the cellular co-receptor (here, CCR5). When the HIV-1 envelope encounters the cell receptors, the released gp120 V3 loop docks into the cellular co-receptor binding site. We envisioned that a bifunctional molecule that has gp120 and CCR5 targeting components would be able to bridge the envelope-CCR5 encounter complex. This kind of complex has not been resolved at

high resolution. However, structural information is available for the individual components.[25, 26] Since PTs target the CD4 binding area of gp120, we measured the distance between the CD4 binding (residue Asp368) site and the tip of the released V3 loop (**Figure 1**, generated from pdb code 2QAD[27]). This distance represents the hypothetical minimal linker length required to tether gp120 and CCR5 inhibitors together, in a way that mimics the encounter complex.

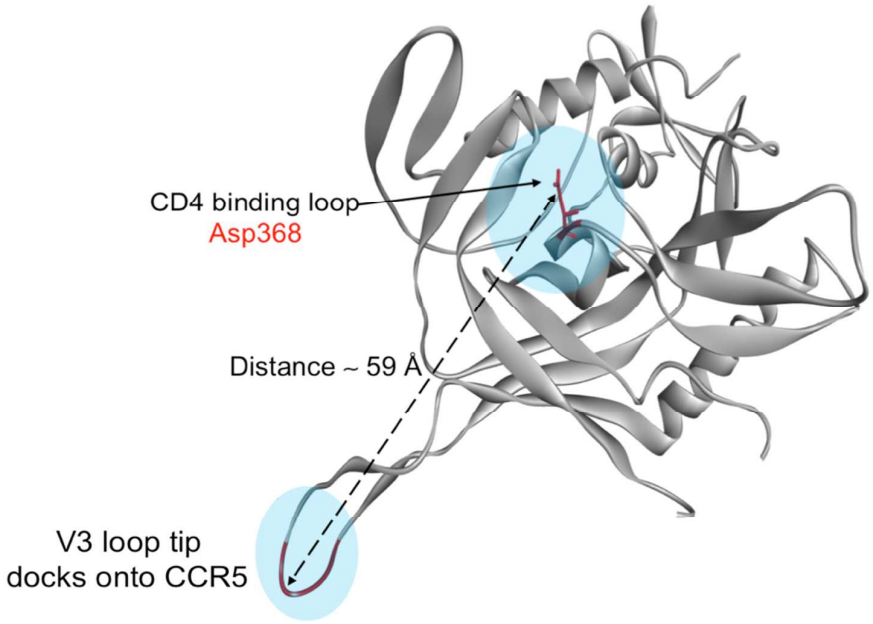

Figure 1. Geometry of gp120 protein, showing the distance between the CD4 binding site and the released V3 loop tip (pdb code 2QAD[27]).

We also examined the possible positions for chemical ligation through modeling of the inhibitors in the context of their individual protein targets (**Figure 2**), in order to avoid any unexpected reduction in potency. As shown in **Figure 2 left**, the UM15 N-terminal (protonated) residue is in a solvent-exposed moiety. On the other hand, the fluorine atom of LJC240 (**Figure 2 right**) is well solvated and actually can displace water of the crystal structure of the CCR5 receptor. This docking result, combined with prior structure-function

relationships in LJC240-derived CCR5 inhibitors[15], argues that structural variation replacing the fluorine atom should be tolerated.

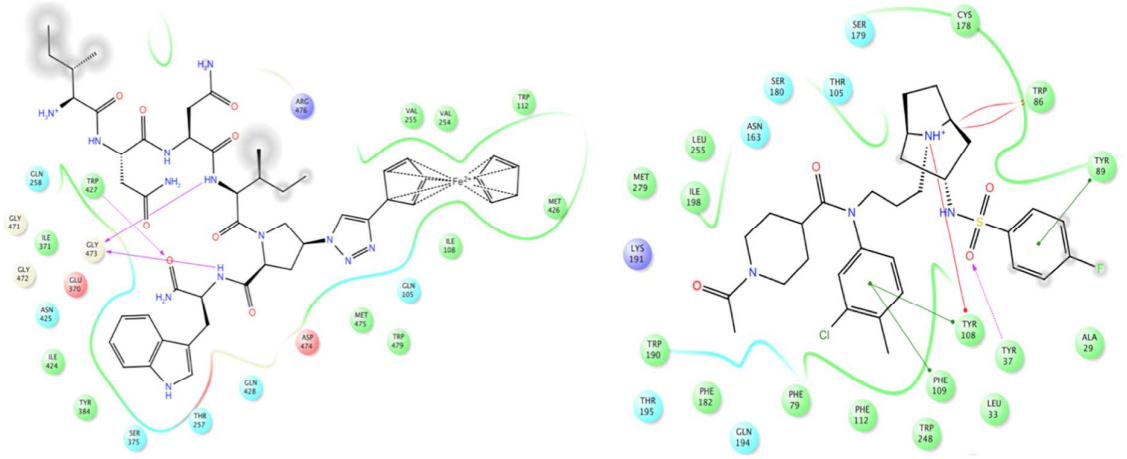

Figure 2. Interaction maps of UM15 (left) docked within gp120 of the HIV-1 envelope (pdb code: 5FUU[28]) and LJC240[15] (right) docked into the CCR5 structure (pdb code: 4MBS[26]). The grey circles represent the solvated (solvent exposed) moieties.

Based on the predicted topology presented above (**Figures 1 and 2**), we envisioned a linker of approximately 59 Å would be required to tether the UM15 N-terminal with the fluoro-phenyl ring. Hydrophilicity built into the linker was predicted to help keep the two components apart and avoid any non-specific hydrophobic interactions with either of the target proteins. We chose 4 units of amino-ethoxy-ethoxy acetic acid as the linker (hereafter referred to as L4) as it would provide the distance based on bond length measurements.

We employed solid phase synthesis to build the L4-UM15 precursor. We also synthesized a modified version of LJC240 (compound **10**, **Figure 3**) in which the fluorine atom (**Figure 2**) was replaced by a carboxylic group to enable ligation with the amino group of the L4-UM15 N-terminus (**Figure 4**). The coupling reagents of HBTU/HOBt and DIEA were selected for the amide-coupling, followed by on-resin click reaction to form the triazole component on the UM15-azido-Pro residue (**Figure 4**).

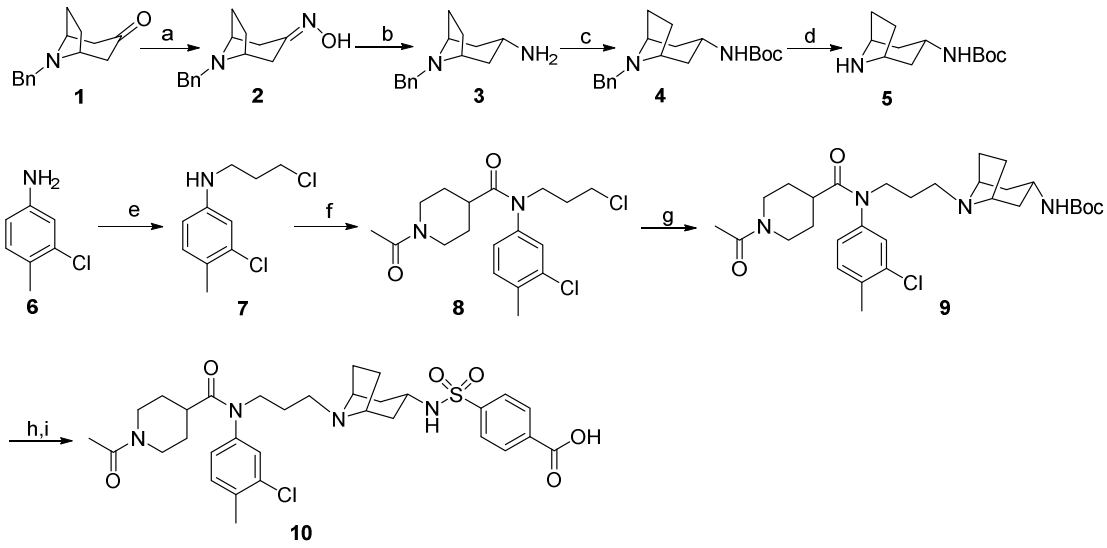

Figure 3. Synthesis of co-receptor inhibitor LJC240-COOH (**10**). *Reagents and conditions*: (a) NH_2OH•HCl, $NaHCO_3$, $EtOH/H_2O$, rt; (b) Na, pentanol, reflux; (c) $(Boc)_2O$, TEA, THF, rt; (d) 10% Pd/C, HCO_2NH_4, Methanol, reflux; (e) 1-bromo-3-chloropropane, KI, TEA, DMF, rt; (f) 1-acetylpiperidine-4-carboxylic acid, $SOCl_2$, TEA, DCM, rt; (g) **5**, KI, K_2CO_3, MeCN, reflux; (h) HCl, Methanol, rt; (i) 4-(chlorosulfonyl)benzoic acid, Na_2CO_3, dioxane/H_2O, rt.

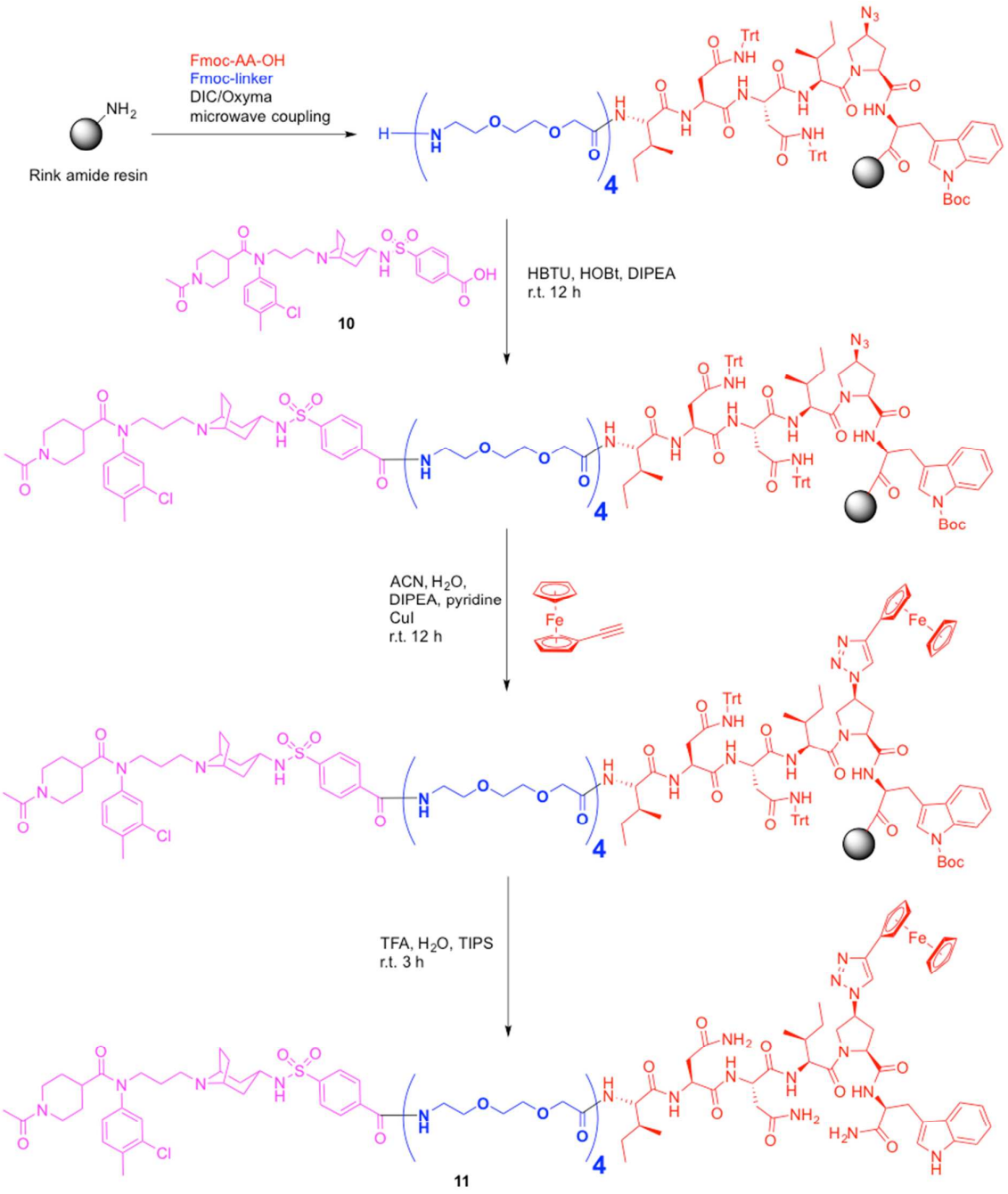

Figure 4. Solid phase synthesis of chimera **11**. Liberty blue microwave synthesizer was used for the assembly of the L4-UM15 precursor segment. The latter was joined with LJC240 free acid (**10**) followed by ferrocenyl triazole formation using click reaction, leading to the final chimera (**11**).

2. The Bifunctional Chimera Displays Potent Neutralization of HIV-1 Infection

We measured the antiviral potency of the bifunctional chimera in a cell infection inhibition assay. Pseudotyped viruses bearing the BaL.01, JR-FL and YU2 envelope proteins, and

carrying a luciferase reporter gene were incubated with serially diluted chimera for 30 minutes at 37 ºC and then added to human osteosarcoma (HOS) cells expressing CD4 and CCR5 (HOS.T4.R5). Following completion of the infection inhibition assay, the cells were lysed and monitored for luciferase activity. UM15 and LJC240-L4 (with the same L4 linker used for the chimera) served as controls for the experiment since they best represent the parental molecules that make up the chimera. LJC240-L4-UM15 (**11**) displayed sub-nanomolar to low nanomolar inhibition of HIV-1 envelope-pseudotyped viruses (**Figure 5**). The chimera had improved potencies that ranged from > 2 fold (YU2) to > 50 fold (BaL.01) greater than the most potent parental component, LJC240-L4. We also evaluated an additional control of a 1:1 non-covalent mixture of UM15 and LJC240-L4 (against the tier-2 JRFL pseudotyped virus) which would mimic the molar ratio between the inhibitors in the chimera, to determine whether the covalent attachment resulted in a potential synergy and increased the potency beyond that of the combination of the individual inhibitors. Indeed, the bifunctional chimera was more potent (4 nM) than the 1:1 mixture (34 nM, **Figure 5B**), thus demonstrating the value of the covalent attachment on potency compared to the sum of its parts.

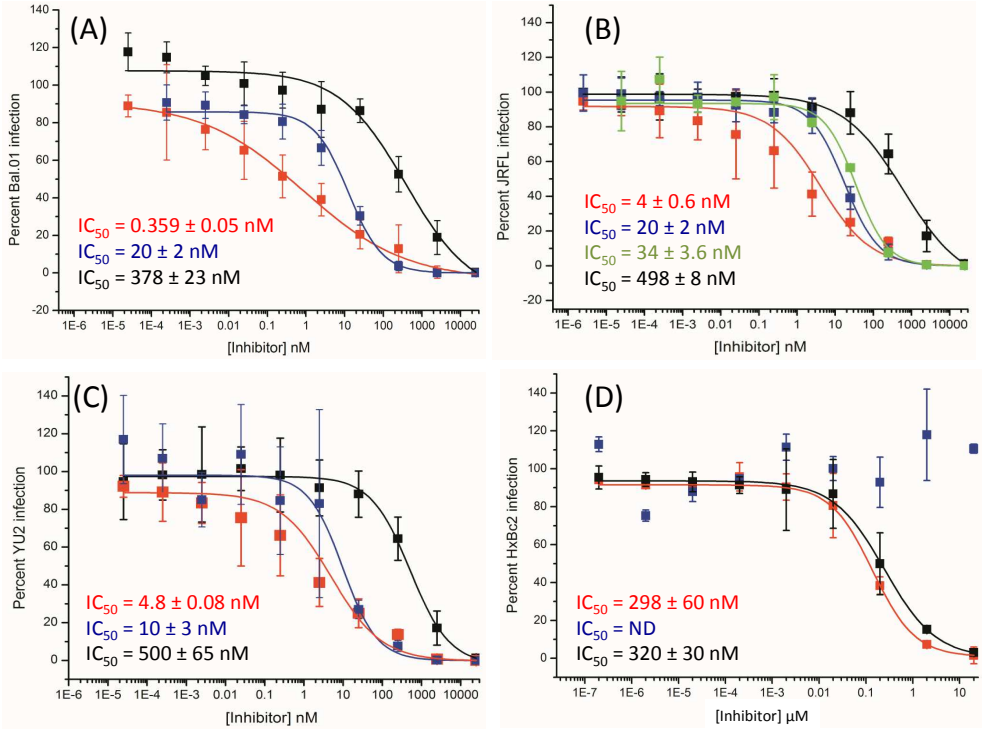

Figure 5. Enhanced neutralization of HIV-1 Env-pseudotyped viruses (A) Bal.01; (B) JRFL; (C) YU2; and (D) HxBc2 as an example of X4 tropic virus by the bifunctional chimera (red), UM15 (black), LJC240-L4 (blue), 1:1 mixture of UM15 and LJC240-L4 (green). ND = not determined.

2.1. Synergistic effect of the covalent chimera

To further define the value of the covalent attachment of UM15 with LJC240-L4 versus the non-covalent mixture, we performed a quantitative synergy analysis. Initially, we evaluated the non-covalent mixtures against Bal.01 HIV-1 strain (due to ease of virus production and assay handling) based on their individual activities reported in **Figure 5**. Interestingly, both UM15 and LJC240-L4 showed ~ 7-fold improved potency in presence of each other (**Figure 6A**); UM15 showed IC_{50} value of 56 nM in the mixture compared to 378 nM alone (**Figure 5A**), while LJC240-L4 showed IC_{50} value of 2.9 nM in the mixture (**Figure 6A**) compared to 20 nM alone (**Figure 5A**). The IC_{50} value obtained for the covalent chimera in the same assay (0.86 nM, **Figure 6A**) clearly showed a strong increase in potency *vs* the noncovalent mixture. These results argue for the value of the covalently joining the two inhibitors

together, further confirming the difference with the 1:1 non-covalent mixture (**Figure 5B**). Representation of the data by an isobologram [29] (**Figure 6B**) shows the synergy between the non-covalent mixture (1:30 molar ratio of UM15:LJC240-L4) when we plotted the 50% inhibition of the mixture (red dot in **Figure 6B**), compared to the individual IC_{50} values of the separate inhibitors (connected by the blue line **Figure 6B**). Interestingly, plotting the 50% inhibition by the covalent chimera **11** (green dot in **Figure 6B**) shows the even stronger synergistic effect of the latter.

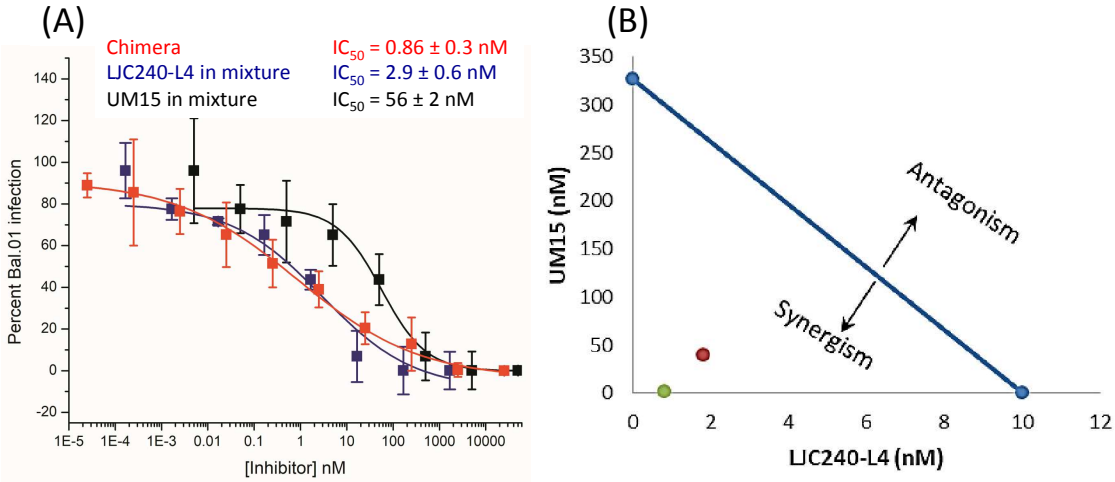

Figure 6. (A) Synergy assay results between UM15 and LJC240-L4 against HIV-Bal.01; IC_{50} values (blue for LJC240-L4 and black for UM15) are the effective inhibitory concentration of the individual component in the mixture, the chimera **11** (red) was also included in the experiment. (B) Isobologram representation of UM15/LJC240-L4 combination; the blue line connects the IC_{50} values of the two inhibitors, the red dot is the effective concentration of the non-covalent mixture (1:30 ratio which achieved 50% inhibition) whereas the green dot is the effective concentration of the covalent chimera **11**.

3. Individual Components of the Chimera Retain Activity

In order to confirm that the covalent attachment of the inhibitors did not interfere with the ability of each molecule to bind to its respective target in the virus-cell interface, we performed a series of experiments to measure the magnitudes of the peptide triazole and co-receptor inhibitor functions of the bifunctional chimera.

3.1. Activity against X4-tropic HIV

Firstly, we performed an infection inhibition assay with HxBc2 (**Figure 5D**), an X4-tropic virus, on HOS cells expressing CD4 and CXCR4 (HOS.T4.X4). By using an X4-tropic virus on X4-expressing cells, we ruled out contribution of the co-receptor inhibitor towards the potency of the chimera. As expected, the bifunctional chimera potency was nearly identical to the UM15 control (**Figure 5D**), thereby demonstrating that the UM15 component of the chimera retained full activity.

*3.2. Chimera **11** retains full gp120 dual antagonism*

Surface Plasmon Resonance (SPR) was carried out to further confirm retention of the UM15 part gp120-binding efficiency. Both soluble CD4 and 17b (a gp120-targeting antibody that stabilizes the bridging sheet) were immobilized separately on sensor chip surfaces, and gp120 was flowed across in increasing concentrations of inhibitor to assess binding. The binding of the bifunctional chimera was again equivalent to the UM15 control (**Figure 7**).

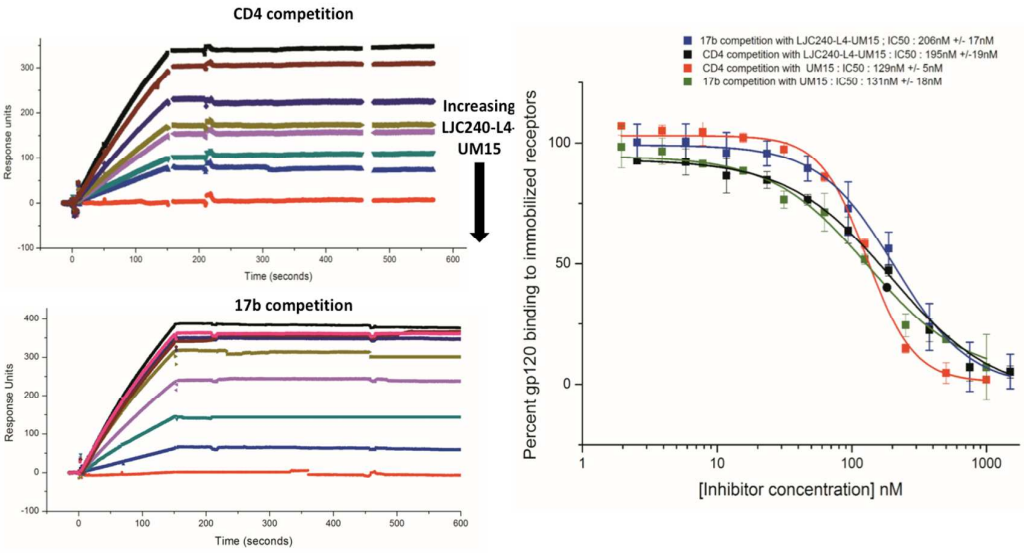

Figure 7. Efficacy of chimeric inhibitor for gp120 protein ligand binding determined by SPR gp120 competition analyses. (Left) Representative sensorgrams showing dose dependent inhibition of monomeric YU2 gp120 binding to the receptors CD4 and 17b by LJC240-L4-UM15. (Right) Dose response curves derived from inhibition of YU2 gp120 binding sensorgrams by LJC240-L4-UM15 and UM15 (n=3).

These findings confirm previous observations that N-terminal extensions on the peptide do not interfere with pharmacophore binding,[30, 31] and also match the docking model for UM15 (**Figure 2**).

*3.3. Chimera **11** irreversibly inactivate HIV via gp120 shedding*

Western blot analysis was used to detect gp120 shedding function of the peptide triazole component. As observed in infection inhibition (**Figure 5D**) and gp120 binding (**Figure 7**), the shedding ability of UM15 was not affected by the covalent attachment to LJC-240, with the chimera and UM15 both inducing gp120 shedding with similar potencies (**Figure 8**). This argues that the unique irreversible virus inactivation capacity is still retained by the chimeric inhibitor.

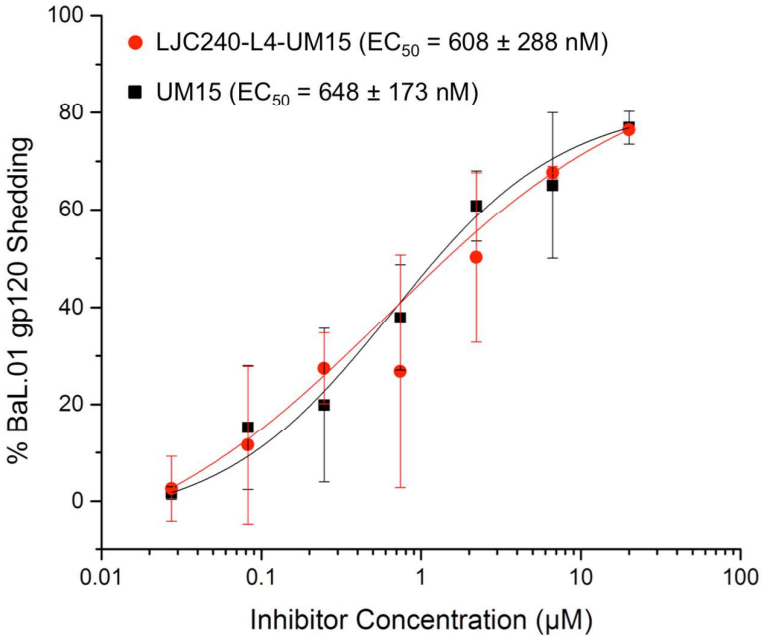

Figure 8. Capacity of the bifunctional chimera LJC240-L4-UM15 to induce gp120 shedding similarly to UM15.

*3.4. Evaluation of Chimera **11** and individual components against CD4-independent HIV*

To further validate the bifunctional approach, we evaluated the chimera **11** and the individual components against an adapted HIV-1 pseudovirus, J1HX, and its CD4 independent mutant N197S. Removal of the glycosylation site at asparagine 197 in the V1/V2 stem was found to be sufficient to enable a conformation that is more primed for CCR5 binding in the absence of CD4, and for HIV-1 entry into CD4-negative cells expressing CCR5.[32] As shown in **Figure 9**, the chimera **11** was functionally active and showed synergy against the parent non-CD4 independent J1HX WT with IC_{50} > 16 fold more active than LJC240-L4 (**Figure 9A**). With the CD4 independent mutant, the individual components remained active: the potency of UM15 component didn't change compared to the WT, arguing that binding of UM15 to gp120 was not disrupted, while the LJC240-L4 component showed ~ 3 fold enhanced potency (**Figure 9B**) compared to the WT. In contrast with the WT J1HX, the chimera **11** was only slightly more active, if at all, than the LJC240-L4 component alone against J1HX N197S virus (**Figure 9B**). The reduced synergistic potency of the chimera **11** observed with J1HX N197S could be due to either [1] masking of the chimera effect by enhanced LJC240-L4 potency or [2] altered dual Env/CCR5 encounter by the chimera components due to rearrangements in the gp120 V1/V2 region. Further investigation will be required to better define the mechanism causing reduced synergy.

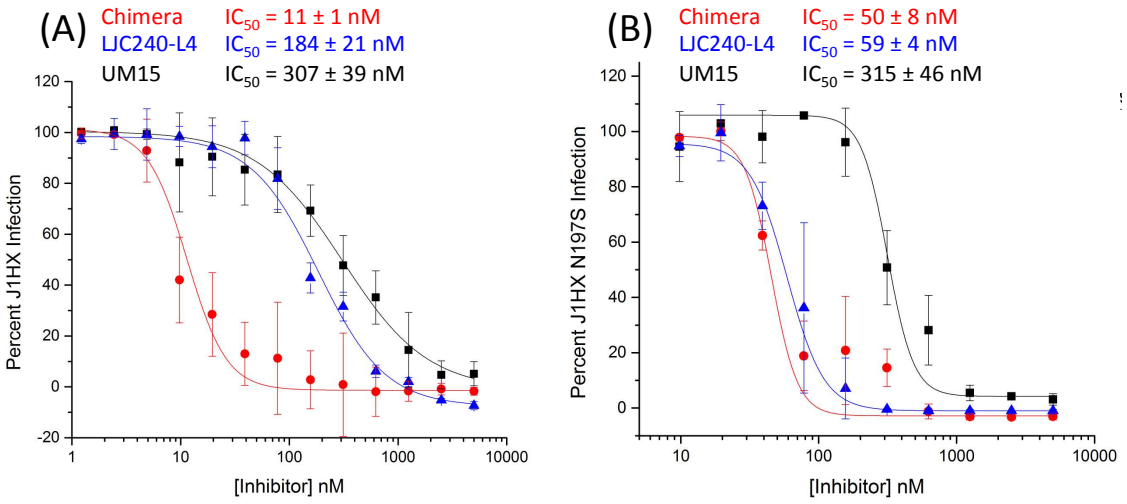

Figure 9. Evaluation of the chimera **11** (red) and the individual components UM15 (black) and LJC240-L4 (blue) against J1HX (A) and the CD4 independent J1HX mutant N197S (B).

*3.5. Chimera **11** retains co-receptor binding efficiency*

The co-receptor inhibitory function of the chimera was assessed, initially using a calcium mobilization assay to determine the extent of antagonism of RANTES function (**Figure 10, top panel**). A comparison of LJC240[15] (**Figure 2**) and LJC240-L4 was included to determine whether the linker would negatively impact antagonistic ability. Indeed, the added linker appeared to interfere with the potency of the molecule, as judged by an activity decrease from 1.59 nM with LJC240 to 27.44 nM with LJC240-L4. No further decrease of function was observed with LJC240-L4-UM15 (**11**), as judged by IC_{50} value of 22.09 nM.

Antagonism of the co-receptor was confirmed using chemotaxis assays with the parent molecules, the linker-containing inhibitor, and the bifunctional chimera. As shown in **Figure 10 bottom panel**, the compounds containing co-receptor inhibitor component, at the IC_{50} values determined in the calcium mobilization assay, all prevented chemotaxis of CEM

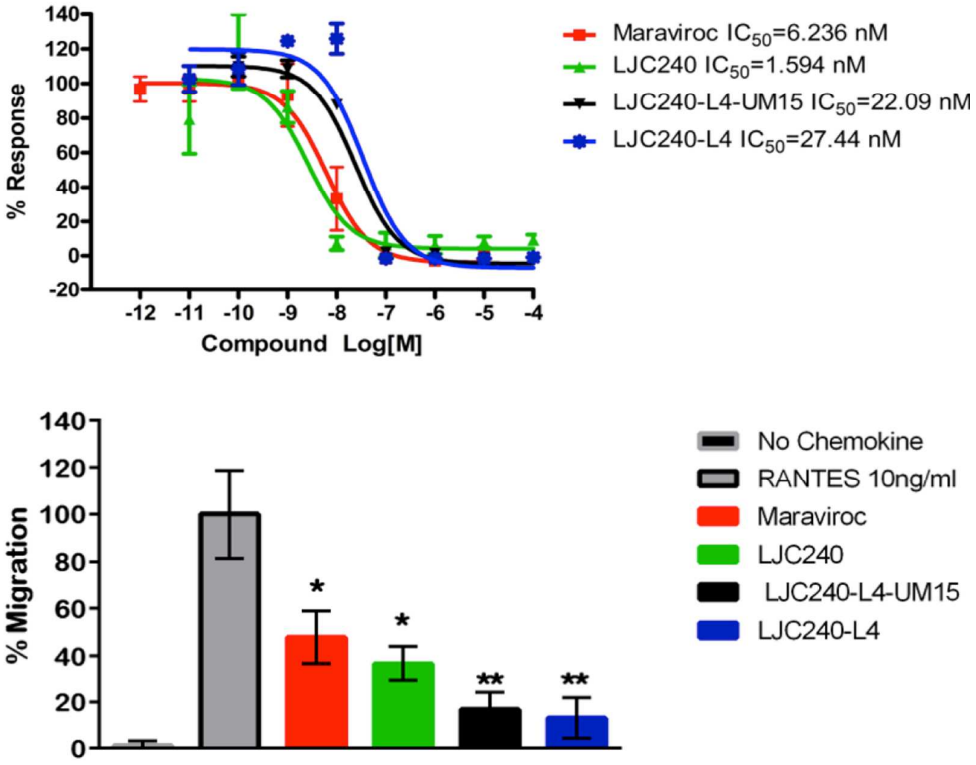

Figure 10. Dose-dependent CCR5 antagonism by the bifunctional chimera and the parent small molecule inhibitors. (**Top**) The extent of inhibition of RANTES (10 nM) stimulation of calcium mobilization was measured for LJC240-containing compounds. Maraviroc was included as a control. (**Bottom**) Chemotaxis inhibition of CEM-CCR5 cells to RANTES by LJC240-L4-UM15. One million CEM CCR5 cells were seeded in the apical chamber of 8um transwell inserts and chemoattraction was induced using RANTES (10 ng/ml) in the presence or absence (control, "No Chemokine") of the inhibitors maraviroc (MRVC), LJC240, LJC240-L4, or the inhibitor-peptide triazole chimera, LJC240-L4-UM15 at the IC_{50} value for each compound. Data are presented as cells recovered in the basolateral chamber post incubation, normalized to cells migrating to RANTES in the absence of inhibitor. Two-way ANOVA was used to compare the inhibitor treated groups to the RANTES only control group and Student's T- test was used to compare individual groups. Error bars represent mean ± SEM. *=p≤ 0.05, **p ≤0.01. These data are representative of 2 independent experiments.

CCR5 cells to RANTES chemokine in a transwell assay. *In vitro* cell toxicity was measured post incubation, and the inhibitors did not lead to cell death measured in the apical and basolateral chambers post treatment (data not shown). These results support the finding that the bifunctional chimera retains the function of antagonizing the CCR5 co-receptor.

4. Cytotoxicity and HIV specificity

To assess cellular safety and HIV specificity, we evaluated the chimera (**11**) in a cytotoxicity WST assay as well as the activity against Acute Murine Leukemia Virus (AMLV). As shown in **Figure 11**, the chimera **11** did not show any cytotoxicity nor any activity against AMLV at the concentration range used.

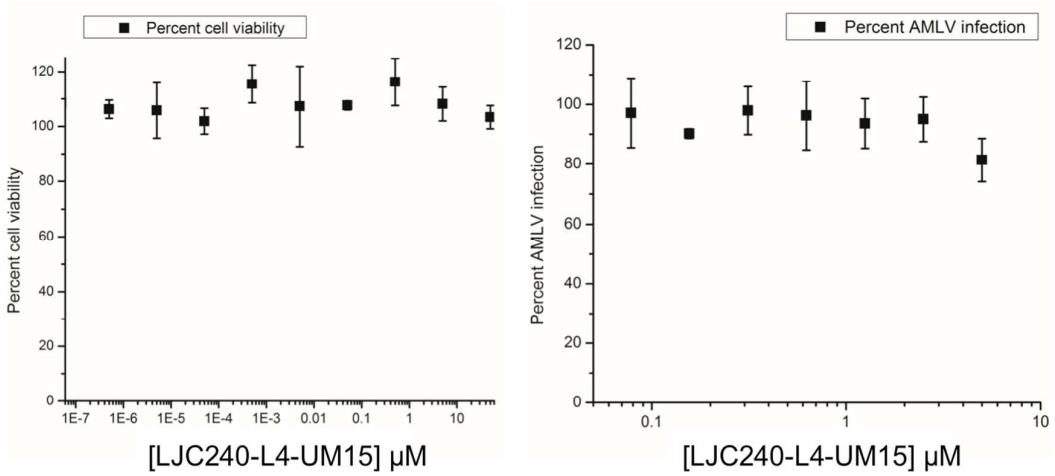

Figure 11. Cytotoxicity evaluation of chimera **11** (left) and evaluation against AMLV (Right).

DISCUSSION

In this work, we engineered a covalent bifunctional chimera capable of inhibiting HIV cell infection through a combination of effects on both sides of the virus-host cell interface. A linker designed to span the distance between the Env and the co-receptor was utilized to join the peptide triazole and the CCR5 antagonist. The first prototype bifunctional chimera generated, namely LJC240-L4-UM15 (**11**), not only displayed enhanced inhibitory potency compared to a 1:1 (mole/mole) non-covalent mixture of the parent molecules that make up the chimera, but also showed better synergistic effect compared to the non-covalent mixtures in a quantitative synergy analysis. This potency was made possible because each component of the chimera is able to function coordinately despite the covalent attachment to the other.

The observed synergistic function of the two inhibitory components of the CoRI-PT chimera argues that both components can function at the same time. This in turn implies a spatial proximity of the gp120 and co-receptor binding sites upon virus-cell encounter. Several hypotheses can be surmised to explain this synergy based on the mode of actions of the chimera components. Since PTs inhibit binding to the co-receptor site likely *via* affecting the release of the V3 loop[33], we envision that as the virus approaches the cell in the presence of the chimera, the PT part of the chimera can dock onto the virion Env, inhibiting CD4 attachment and altering the and V3 loop/CCR5 epitope release mechanism. However, the chimera has another exposed scaffold, which is the CCR5 blocker. This CCR5 blocker brings the Env-chimera complex closer to the cell to dock onto the CCR5 protein. The net result of this mechanism is locking the virus-cell complex in an arrested configuration, leading to blocking the infection and later on causing gp120 shedding by PT domain function. In other words, the chimera CCR5-L4 inhibitor part can act as a false V3 loop, bringing the virus closer to the cell, not for initiating infection, rather to be blocked. On the other hand, the entropic advantage from the tethered hybrid over the separate two components might be one cause of the synergistic effect.[34] When the chimera binds to one site/protein at the cell-virus interface, much of the entropy cost of binding to the second site/protein has already been paid. Thus, the free energy of binding for the chimera is not the sum of the free energies of the two components because of entropy, leading to a synergistic potency. Importantly, the shedding function of the chimera was demonstrated in this work. Nonetheless, the sequence of bifunctional chimera binding events at the cell-virus interface remains speculative at present.

While other covalent chimeras have been designed that target HIV-1 infection[35-40], the prototype chimera LJC240-L4-UM15 (**11**) is unique in the added value of irreversible inactivation the virus. Previously, chimeric inhibitors have been reported that target [1] two

sites on the HIV-1 Env protein alone[36, 38, 39], [2] CD4 and Env gp41[35] and [3] Env gp41 and co-receptor.[37, 40] The latter findings have demonstrated the feasibility of bifunctional engagement of both virus Env and host cell receptors. Since CCR5 and CXCR4 co-receptors can heterodimerize with each other[41], the CCR5-targeting CoRI-PT chimera reported in the current work has an additional potential to bind to the CCR5 in the heterodimer and neutralize X4-tropic virus by Env inactivation through the PT domain (which is active against both X4- and R5-viruses) before CXCR4 encounter.

Bifunctional chimeras of the CoRI-PT type have an important advantage in avoiding virus resistance, by combining components that can function synergistically or separately against evolving viruses and hence challenging the virus to combine escape to two different inhibitory functions coordinately. Analogously with most if not all virus protein targeting antagonists, mutational escape of the Env-binding PT component can occur[31]. Further, even though CoRIs target a host cell protein *vs* a virus protein, HIV-1 resistance mutations to co-receptor antagonists have been observed to occur by forming binding sites on the virus Env protein that can bind the antagonist-bound form of the co-receptor and in this way infecting cells in the presence of CoRIs.[42] We envision that, since the CCR5 antagonist in the LJC240-L4-UM15 chimera (**11**) is attached to a relatively large peptide and linker moiety, it would be difficult for virus to bind the chimera-armed co-receptor due to increased spatial blockade. But, even if the virus could overcome this blockade, the added challenge of escaping the PT component of the chimera would improve the ability of the chimera to avoid overall inhibitor escape.

The results of the current work open up both future chimera design opportunities and potential for expanded functional utility. The chimeric inhibitor **11** presented in this work serves as a prototype for advancing more drug-like chimeric inhibitors. The recent discovery of macrocyclic PTs (cPTs)[19, 43], combined with existing[44] and newly discovered CXCR4-

targeting small molecules[45], provide the potential to develop drug-like and protease-resistant CoRI-cPT variants that will target both CCR5 and CXCR4 cellular infection with improved bioavailability. Increased understanding about the structural mechanism of action of the chimeras will be helpful to guide future chimera design. As the latter is progressing, the relatively small size of such chimeras will make it feasible to investigate whether these could inhibit not only virus-cell infection but also cell-to-cell transmission.

CONCLUSIONS

In summary, we have designed and produced a fully synthetic bi-functional chimeric inhibitor that can target both sides of the HIV-cell interface. One component blocks the viral envelope and the second component blocks the cellular co-receptor CCR5. The chimera showed synergistic potency compared to the non-covalent mixture(s) of the individual components. This result demonstrates the ability of making potent, fully synthetic HIV-1 inhibitors by simultaneously targeting the virus Env and its cellular chemokine receptors.

EXPERIMENTAL SECTION

Docking of LJC240 onto the CCR5 receptor

The recently solved crystal structure of CCR5 bound to inhibitor Maraviroc was used (pdb code 4MBS[26]. The pdb file was downloaded from the Protein Data Bank and prepared with the protein preparation wizard in Maestro 9.9 (Schrödinger Suite 2015; Schrödinger, LLC). Before docking LJC240, The docking procedures were validated where the co-crystallized Maraviroc was docked onto the receptor structure (using Glide-XP docking protocol) and showed similar pose to the crystallographically solved bound state (heavy atoms RMSD = 0.31 Å, data not shown) and had a calculated receptor-Maraviroc interaction energy value of ~ -33.2 kcal/mol as calculated using Szybki 1.8.0.2 (Openeye Scientific Software, Santa Fe,

NM. http://www.eyesopen.com). LJC240 was built and prepared using the builder and LigPrep tools in Maestro 9.9[46]. The inhibitor LJC-240 was then docked onto the CCR5 receptor using the same Glide-XP protocol. This yielded a stable low energy pose (**Figure 2**) with a calculated receptor-ligand interaction energy of ~ -27.1 kcal/mol (calculated using Szybki 1.8.0.2, Openeye Scientific Software, Santa Fe, NM. http://www.eyesopen.com). The docking showed the fluorophenyl moiety of the inhibitor to be the most solvent exposed part, with the least important interaction. This was in agreement with the SAR studies (Long Lab) that changes in this part of the molecule can be tolerated.

Docking of UM15 onto the gp120 protein

Peptide UM15 was built and docked onto gp120 chain A of the SOSIP Env trimer (pdb code 4NCO[25], structure as previously described[47] using the InducedFit docking protocol[48]. The N terminal of the UM15 was shown to be well solvated (**Figure 2**) and can be used as an extension point for the Chimera synthesis.

Chemical synthesis

General Information

The starting materials were obtained from commercial sources, such as Adamas-beta, Sigma-Aldrich, J&K, TCI and Chem-Impex, which were used without further purification. Unless otherwise specified, all reactions were carried out in oven-dried glassware with magnetic stirring. All reagents were weighed and handled in air at room temperature. Unless otherwise stated, commercially obtained materials were used without further purification. Column chromatography was performed on silica gel (200-300 mesh). The column output was monitored by TLC on silica gel (100-200 mesh) precoated on glass plates (15 x 50 mm), and spots were visualized by UV light at 254 nm. All new compounds were characterized by ^{1}H NMR, ^{13}C NMR and low/high resolution mass spectroscopy. NMR spectra were recorded on

a Brucker AVANCE III 400 NMR spectrometer. Chemical shifts for proton magnetic resonance spectra (^{1}H NMR) were quoted in parts per million (ppm) referenced to the signals of residual chloroform (7.26 ppm) or methanol (3.30 ppm). All ^{13}C NMR spectra are reported in ppm relative to deuterochloroform (77.23 ppm) or methanol (49.00 ppm). The following abbreviations were used to describe peak splitting patterns when appropriate: br = broad, s = singlet, d = doublet, t = triplet, q = quartet, m = multriplet, dd = doublet of doublet. Coupling constants, *J*, were reported in hertz unit (Hz). Mass spectra were recorded using an ESI ion source unless stated otherwise. All melting points were measured using a BÜCHI 510 melting point apparatus. The yields in this paper refer to isolated yields of compounds estimated to be ≥95% pure as determined by ^{1}H NMR. Unless otherwise specified, the purity of all new compounds was determined by analytical HPLC on Agilent Technologies 1260 Infinity with Aglient ZORBAX 3.5 μM SB-phenyl column (4.6 × 75 mm) in one solvent system (solvent A, 0.02% TFA in water; solvent B, 0.02% TFA in acetonitrile) with gradient indicated below; flow rate, 1.5 mL/min; UV detector, 210 and/or 254 nm. Method: 5% B to 90% B in 12 min, 90% B for 3 min.

Synthesis of 8-Benzyl-8-aza-bicyclo[3.2.1]octan-3-one oxime (2)[49]: A mixture of 8-benzyl-8-aza-bicyclo[3.2.1]octan-3-one (5.00g, 23.2mmol), hydroxylamine hydrochloride (1.78g, 25.6 mmol) and $NaHCO_3$ (2.54g, 30.2mmol) was stirred in EtOH/H_2O (60 mL, v:v=1:1) for 18 hours. The reaction mixture was filtered and the residue was washed with water, dried to afford the compound **2** as a white solid (3.24g, yield 61%), m.p. 118-120 ^{o}C. ^{1}H NMR (400 MHz, $CDCl_3$) δ 7.43 (d, *J* = 7.2 Hz, 2H), 7.38 – 7.32 (m, 2H), 7.32 – 7.29 (m, 1H), 3.70 (s, 2H), 3.43 – 3.34 (m, 2H), 3.02 (d, *J* = 15.5 Hz, 1H), 2.66 – 2.59 (m, 1H), 2.31-2.23 (m, 1H), 2.18-2.05 (m, 1H), 2.10 – 2.00 (m, 2H), 1.66 (t, *J* = 7.9 Hz, 1H), 1.56 (t, *J* = 7.6 Hz, 1H). ^{13}C

NMR (151 MHz, CDCl3) δ 157.0, 139.3, 128.6, 128.3, 127.0, 58.5, 57.8, 55.6, 37.3, 31.3, 27.6, 26.7. HRMS (ESI) Calcd for $C_{14}H_{19}N_2O$ $[M+H]^+$: 231.1492, found 231.1489.

Synthesis of exo-8-Benzyl-8-aza-bicyclo[3.2.1]oct-3-ylamine (3)[50]: A solution of the compound **2** (3.00 g, 13.0 mmol) in pentanol (50 mL) was heated under reflux. Sodium (3.59 g, 156.3 mmol) was added portionwise over 2.5 hours. The reaction was then heated under reflux for a further 2 hours, then cooled in an ice bath. Water was added until no more hydrogen gas was evolved. The mixture was acidified using 6N aqueous hydrochloric acid and the phases separated. The organic layer was extracted with 6N aqueous hydrochloric acid, the combined aqueous extracts were basified to pH 12 with sodium hydroxide pellets and the aqueous solution extracted with ethyl acetate. The combined organic solutions were dried with $MgSO_4$, filtered and evaporated under reduced pressure to afford the compound **3** as colorless oil (1.91 g, yield 68%). ^{1}H NMR (400 MHz, $CDCl_3$) δ 7.45 – 7.36 (m, 2H), 7.30-7.25 (m, 2H), 7.26 – 7.19 (m, 1H), 3.63 (s, 2H), 3.38 – 3.23 (m, 3H), 2.09 – 1.97 (m, 2H), 1.96 – 1.80 (m, 4H), 1.67 – 1.53 (m, 2H). ^{13}C NMR (126 MHz, CDCl3) δ 138.2, 128.4, 127.9, 126.7, 57.5, 54.5, 43.6, 35.7, 26.1. HRMS (ESI) Calcd for $C_{14}H_{21}N_2$ $[M+H]^+$: 217.1699, found 217.1704.

Synthesis of *exo*-(8-Benzyl-8-aza-bicyclo[3.2.1]oct-3-yl)-carbamic acid *tert*-butyl ester (4)[51]: A mixture of compound **3** (3.00 g, 13.9 mmol), Boc_2O (3.33g, 15.3 mmol) and TEA (3.9 mL, 27.7 mmol) was stirred in THF (52 mL) for 18 hours. The reaction mixture was evaporated under reduced pressure. The residue was purified by recrystallization, affording compound **4** as a white solid (4.19 g, yield 95%), m.p. 174-175 ^{o}C. ^{1}H NMR (400 MHz, $CDCl_3$) δ 7.38 (d, J = 7.3 Hz, 2H), 7.32 (t, J = 7.4 Hz, 2H), 7.26- 7.23 (m, 1H), 3.56 (s, 2H), 3.31-3.14 (m , 2H), 2.05-2.00 (m, 2H), 1.84-1.78 (m, 2H), 1.73-1.69 (m, 2H), 1.58-1.50 (m,

3H), 1.43 (s, 9H). ^{13}C NMR (126 MHz, $CDCl_3$) δ 155.3, 140.0, 128.5, 128.2, 126.8, 79.2, 58.7, 56.1, 42.8, 38.7, 28.4, 26.5. HRMS (ESI) Calcd for $C_{19}H_{29}N_2O_2$ $[M+H]^+$: 317.2224, found 317.2224.

Synthesis of *exo*-(8-Aza-bicyclo[3.2.1]oct-3-yl)-carbamic acid *tert*-butyl ester (5)[52]: A solution of the compound **4** (2.73 g, 8.6 mmol) in methanol (40 mL) was added 10% Pd/C (273 mg, ca.50% water) and HCO_2NH_4 (3.81g, 60.4 mmol), the above mixture was heated under reflux for 15 min. Cooled to room temperature, the reaction mixture was evaporated under reduced pressure. Purification by flash chromatography on silica gel (DCM / methanol = 10:1) afforded compound **5** as a white solid (1.43 g, yield 73%), m.p. 271-272 ^{o}C. ^{1}H NMR (400 MHz, $CDCl_3$) δ 4.80-4.76 (m, 1H), 4.08-4.02 (m, 2H), 2.29 – 2.20 (m, 2H), 2.05 – 1.93 (m, 6H), 1.42 (s, 9H). ^{13}C NMR (126 MHz, $CDCl_3$) δ 169.0, 79.8, 54.7, 41.1, 35.4, 28.3, 26.3. HRMS (ESI) Calcd for $C_{12}H_{23}N_2O_2$ $[M+H]^+$: 227.1754, found 227.1748.

Synthesis of (3-Chloro-4-methyl-phenyl)-(3-chloro-propyl)-amine (7)[53]**:** To a mixture of 1-bromo-3-chloropropane (10.5 mL, 105.9 mmol) in DMF was added KI (586 mg, 3.5 mmol), and the mixture was stirred at room temperature for 30 min, then TEA (19.6 mL, 141.2 mmol) and 3-Chloro-4-methyl-phenylamine (5.00 g, 35.3 mmol) was added and stirred at room temperature for further 72h. The reaction mixture was filtered, and the filtrate was concentrated in vacuum. The residue was diluted with EtOAc, washed with water and brine, dried with $MgSO_4$, filtered, and concentrated in vacuum. Purification by flash chromatography on silica gel (petroleum ether / ethyl acetate = 25:1) afforded compound **7** as yellow oil (5.20 g, yield 68%). ^{1}H NMR (400 MHz, $CDCl_3$) δ 7.01 (d, J = 8.2 Hz, 1H), 6.63 (d, J = 2.4 Hz, 1H), 6.44 (dd, J = 8.2, 2.5 Hz, 1H), 3.65 (t, J = 6.2 Hz, 2H), 3.30 (t, J = 6.6 Hz, 2H), 2.25 (s, 3H), 2.05 (p, J = 6.5 Hz, 2H). ^{13}C NMR (126 MHz, $CDCl_3$) δ 147.0, 134.9,

131.4, 124.4 113.1, 111.7, 42.5, 41.1, 31.8, 18.9. HRMS (ESI) Calcd for $C_{10}H_{14}Cl_2N$ $[M+H]^+$: 218.0498, found 218.0497.

Synthesis of 1-Acetyl-piperidine-4-carboxylic acid (3-chloro-4-methyl-phenyl)-(3-chloro-propyl)-amide (8)[53]: To a solution of 1-acetylpiperidine-4-carboxylic acid (6.75 g, 39.4 mmol) in $SOCl_2$ (40 mL) was stirred for 2 h at room temperature. The reaction mixture was diluted with petroleum ether and filtered to afford the acyl chloride as white solid. Compound **7** (2.87 g, 13.1 mmol) was dissolved in DCM (50 mL), TEA (5.5 mL, 39.4 mmol) and acyl chloride were added, then the mixture was stirred at room temperature for further 2h. The residue was diluted with DCM, washed with water and brine, dried with $MgSO_4$, filtered, and concentrated in vacuum. Purification by flash chromatography on silica gel (petroleum ether / ethyl acetate = 1:1) afforded compound **8** as a white solid (3.74 g, yield 77%), m.p. 101-103 ^oC. ^1H NMR (400 MHz, $CDCl_3$) δ 7.31 (d, J = 8.0 Hz, 1H), 7.18 (d, J = 2.0 Hz, 1H), 6.97 (dd, J = 8.0, 2.1 Hz, 1H), 4.51 (d, J = 13.3 Hz, 1H), 3.78-3.75 (m, 2H), 3.53 (t, J = 6.6 Hz, 2H), 2.87-2.81 (m, 1H), 2.43 (s, 3H), 2.39 – 2.28 (m, 2H), 2.05 (s, 3H), 2.02-1.96 (m, 2H), 1.67 – 1.55 (m, 5H). ^{13}C NMR (126 MHz, $CDCl_3$) δ 174.2, 168.8, 140.9, 136.7, 135.4, 132.1, 128.4, 126.2, 47.7, 45.5, 42.3, 40.7, 39.3, 30.8, 28.8, 28.3, 21.4, 19.8. HRMS (ESI) Calcd for $C_{18}H_{25}Cl_2N_2O_2$ $[M+H]^+$: 371.1288, found 371.1281.

Synthesis of *exo*-1-Acetyl-piperidine-4-carboxylic acid [3-(3-amino-8-aza-bicyclo[3.2.1]oct -8-yl)-propyl]-(3-chloro-4-methyl-phenyl)-amide (9): To a mixture of compound **8** (1.70 g, 4.6 mmol), compound **5** (1.04 g, 4.6 mmol) and KI (760 mg, 4.6 mmol) in acetonitrile was added $NaHCO_3$ (1.15 g, 13.7 mmol), and the mixture was stirred at reflux for 12h. After cooling to room temperature, the mixture was filtered, and the filtrate was concentrated in vacuum. The residue was diluted with EtOAc, washed with water and brine,

dried with $MgSO_4$, filtered, and concentrated in vacuum. Purification by flash chromatography on silica gel (DCM/methanol = 25:1) afforded the product as a white foam (1.72 g, yield 67%). ^{1}H NMR (400 MHz, $CDCl_3$) δ 7.31 (d, *J* = 8.1 Hz, 1H), 7.20 (d, *J* = 1.4 Hz, 1H), 7.08 (d, *J* = 7.7 Hz, 1H), 4.65 – 4.46 (m, 2H), 3.88 – 3.60 (m, 4H), 3.49 – 3.38 (m, 2H), 2.82 (t, *J* = 13.7 Hz, 1H), 2.57-2.50 (m, 2H), 2.40 (s, 3H), 2.36 – 2.25 (m, 2H), 2.03 (s, 3H), 2.00 – 1.95 (m, 2H), 1.84-1.79 (m, 8H), 1.67 – 1.54 (m, 3H), 1.41 (s, 9H). ^{13}C NMR (126 MHz, $CDCl_3$) δ 174.3, 168.8, 155.3, 140.7, 136.7, 135.3, 132.1, 128.4, 126.6, 79.5, 59.7, 54.7, 48.9, 47.5, 45.5, 41.8, 40.7, 39.4, 36.8, 28.9, 28.4, 28.3, 25.8, 21.4, 19.8. HRMS (ESI) Calcd for $C_{30}H_{46}ClN_4O_4$ $[M+H]^+$: 561.3202, found 561.3214. Purtiy: 99.8% (t_R=6.63).

Synthesis of 4-8-(3-(1-Acetyl-N-(3-chloro-4-methylphenyl)piperidine-4-carboxamido)propyl)-8-azabicyclo[3.2.1]octan-3-yl)sulfamoyl)benzoic acid (10): To a solution of compound **9** (2.62 g, 4.7 mmol) in methanol, HCl (4.8 M, in methanol) was added, and the mixture was stirred at room temperature for 4h. After concentrating the reaction mixture in vacuum, the residue (1.57 g, 3.4 mmol) was dissolved in 1,4-dioxane (40 mL), then 4-(chlorosulfonyl)benzoic acid (1.50 g, 6.8 mmol) and a solution of Na_2CO_3 (1.08 g, 10.2 mmol) in H_2O (20 mL) were added, and the mixture was stirred at room temperature for 12h. The residue was evaporated in vacuum, washed with mixture of methanol and DCM (DCM/methanol= 9:1), filtered, and filtrate was concentrated in vacuum. Purification by flash chromatography on silica gel (DCM / methanol = 10:1) afforded compound **10** as a white solid (1.22 g, yield 40% for two steps), m.p. 182-184 ^{o}C. ^{1}H NMR (400 MHz, MeOD) δ 8.01 (d, *J* = 8.5 Hz, 2H), 7.82 (d, *J* = 8.5 Hz, 2H), 7.35 (dd, *J* = 8.5, 5.1 Hz, 2H), 7.11 (dd, *J* = 8.1, 2.1 Hz, 1H), 4.35 – 4.26 (m, 1H), 3.86 – 3.79 (m, 2H), 3.78 – 3.70 (m, 1H), 3.67-3.60 (m, 2H), 3.56 – 3.46 (m, 1H), 2.95 – 2.87 (m, 2H), 2.78 (t, *J* = 11.4 Hz, 1H), 2.42-2.36 (m, 1H), 2.31 (s, 3H), 2.29-2.24 (m, 1H), 2.16-2.08 (m, 2H), 1.95 (s, 3H), 1.86 – 1.74 (m, 8H), 1.59 (d,

J = 15.2 Hz, 3H), 1.45 (d, *J* = 16.2 Hz, 1H). ^{13}C NMR (126 MHz, MeOD) δ176.0 (2), 169.7, 143.2, 139.6, 139.0, 136.7, 134.7, 131.9, 129.4, 127.7, 125.9, 125.7, 60.8, 45.9, 44.8, 43.1, 40.0, 38.9, 28.0, 27.5, 23.5, 22.3, 19.3, 18.0. HRMS (ESI) Calcd for $C_{32}H_{42}ClN_4O_6S$ $[M+H]^+$: 645.2508, found 645.2506. Purtiy: 99.5% (t_R=5.61).

Solid Phase Synthesis of LJC240-L4

Rink amide resin (0.1 mmol, 200-400 mesh) was swollen in 10 mL of DMF: DCM (1:1). Fmoc deprotection was achieved using a solution of 20% piperidine/ in DMF. The Fmoc-protected linker (116 mg, 0.3 mmol) was dissolved in DMF, DIEA (124 μl, 0.75 mmol) and HBTU (110 mg, 0.29 mmol) were added and the mixture was vibrated for 30 min at room temperature then added to the reaction vessel, vibrated at room temperature for 4 h. Four units of the linker were installed. LJC240-COOH (**10**, 193 mg, 0.3 mmol) was dissolved in DMF, then DIEA (124 μl, 0.75 mmol), HOBt (41 mg, 0.3 mmol) and HBTU (110 mg, 0.29 mmol) were added, and the mixture was vibrated for 30 min then added to the $(linker)_4$-resin vessel. The reaction vessel was vibrated at room temperature for 12 h. Cleavage was carried out using a cocktail of trifluoroacetic acid/ethanedithiol/H_2O (4.75/0.125/0.125 v/v) for 2h at room temperature. Cleaved compound solution was concentrated under a gentle N_2 stream, then dissolved in ACN/H_2O. Crude product was purified by semi-preparative HPLC on an EasySep^{TM}-1050 with XBridge™ Prep C18 reversed-phase column (19 × 150 mm, ACN/H_2O/0.1% TFA, t_R=17.7 min (gradient: 10−90% ACN over 30 min; flow rate of 4 mL/min) and finally evaporated in vacuum to yield ideal product. ^{1}H NMR (400 MHz, MeOD) δ 8.06 – 7.99 (m, 4H), 7.51 – 7.46 (m, 2H), 7.24 (dd, *J* = 7.9, 2.0 Hz, 1H), 4.45 (d, *J* = 13.9 Hz, 1H), 4.02 (s, 4H), 3.99 (s, 3H), 3.91 – 3.75 (m, 3H), 3.75 – 3.64 (m, 17H), 3.62-3.55 (m, 6H), 3.51 – 3.39 (m, 5H), 3.06 – 2.98 (m, 2H), 2.95 – 2.82 (m, 2H), 2.72 (s, 2H), 2.57 – 2.49 (m, 1H), 2.44 (s, 3H), 2.43 – 2.38 (m, 1H), 2.29 – 2.21 (m, 2H), 2.08 (s, 3H), 2.06 (s, 1H), 2.02 – 1.87 (m, 7H), 1.77 – 1.54 (m, 5H), 1.38 – 1.28 (m, 4H). ^{13}C NMR (126 MHz,

MeOD) δ 176.0, 174.0, 171.0, 169.6, 166.9, 143.8, 139.6, 137.8, 136.7, 134.7, 131.8, 127.7, 127.6, 126.2, 125.9, 70.1 (4), 69.7 – 69.1 (8), 68.9 – 68.5 (4), 61.2, 45.8, 44.8, 43.1, 40.0, 39.2, 38.9, 37.9, 36.4, 33.5, 28.1, 27.5, 23.4, 22.2, 19.3, 18.0. HRMS (ESI) Calcd for $C_{56}H_{87}ClN_9O_{17}S$ $[M+H]^+$: 1224.5624, found 1224.5627. Purtiy: 99.0% (t_R=8.47).

Solid Phase Synthesis of LJC240-L4-UM15 (11)

Solid Phase synthesis of resin-bound linker-PT

Using Fmoc-based synthesis strategy, the following sequence was assembled using microwave assisted coupling: $(linker)_4$-ile-asn-asn-ile-AzidoPro-trp-resin. Resin = rink amide resin (100-200 mesh size), 0.25 mM synthesis scale. Activation scheme (1 mL 0.5 M DIC/0.5 mL 0.5 M Oxyma) was used. Deprotection of Fmoc groups by 5 mL 20% piperidine+0.1 M HOBt in DMF.

Coupling LJC-240-COOH to the Linker-PT-resin

The $(linker)_4$-peptide-resin was swollen by soaking in 10 mL of DMF:DCM (1:1) . 1.1 equivalent of LJC-240-COOH (**10**) + 2.2 equivalent HBTU + 2.2 equivalent HOBt + 4.4 equivalent DIPEA were added to the reaction vessel. The vessel was vibrated for 10 h at room temperature and reaction monitored by Kaiser test until negative (no blue color) test observed. The resin-bound complex was then filtered; resin was washed thoroughly by DMF, Methanol and DCM.

Click reaction of the alkyne (ethynylferrocene) with the azide group on Pro residue

The resin-bound fusion was mixed with (5 mL ACN, 4 mL H_2O, 1.06 mL DIPEA and 0.53 mL pyridine + 5 equivalent ethynylferrocene), and the reaction vessel was vibrated at room temperature for 12 h. The resin-bound product was washed thoroughly by 5% HCl (2 x 50 mL), DMF (2 x 50 mL) and DCM (2 x 50 mL).

Cleavage of the fusion from resin and deprotection of peptide side chains

The resin-bound product was mixed with a chilled cleavage mixture, 20 mL (95% TFA, 2.5% H_20, 2.5% TIPS) and vibrated for 2.5 h at room temperature. The reaction mixture was filtered and the leftover resin was washed with 10 mL of the cleavage mixture. The acidic filtrate was concentrated under a gentle N_2 stream. Pre-cooled ether (30 mL) was added to the residue, after rigorous vortexing and centrifugation, the ether layer was decanted. This ether-washing step was repeated 2-3 times until the ether layer was no longer colored. The residue was then vacuum dried, re-dissolved in ACN/H_20/0.1% TFA mixture for RP-HPLC purification (Waters HPLC, absorption at 210 nm) using Waters C18 prep column. The pure HPLC fractions ($\geq$ 97% purity as judged by analytical HPLC; 5% to 95% ACN + 0.1%TFA in 40 min) were lyophilized to give the chimera **11** as a pale yellow powder (65% yield calculated based on cleavage of 0.5 g resin). The MALDI-TOF determined mass of the purified chimera was found to be 2212.75 Da, compared to calculated mass of 2211.96 Da.

Production of HIV-1 Envelope Pseudotyped Virus

Recombinant envelope pseudotyped viruses were prepared by co-transfection of an Envelope expression plasmid, either JR-FL (R5-tropic) or HxBc2 (X4-tropic), with an HIV-1 viral backbone plasmid encoded with a luciferase gene and lacking Env, pNL Luc AM.[54] A combination of 4 mg of Env and 8 mg of backbone DNA were transfected into 293T cells using PEI (Fisher Scientific) as a transfection reagent. Cell supernatant containing the recombinant viruses were collected after 48 to 72 hours and purified through a 6-20% iodixanol (Sigma Aldrich) gradient to remove free viral proteins and exosomes. The gradient was performed at 4°C for 2 hours at 30,000 rpm (SW41 rotor, Beckman ultracentrifuge). The fractions were collected following the spin, validated as previously described and at stored at -80°C until needed.

Infection Inhibition Assay

The LJC240-L4-UM15 (**11**) bifunctional chimera was evaluated for potency using a standard pseudoviral assay.[54, 55] Briefly, envelope pseudotyped viruses were treated for 30 minutes at 37 °C with inhibitor and then added to HOS cells expressing both CD4 and an appropriate co-receptor depending on the assay. The infection was carried out for 24 hours before a medium change was performed to remove any residual virus or inhibitor. Production of reporter luciferase was allowed to continue for an additional 24 hours before lysing the cells with passive lysis buffer (Promega). Cell lysates were transferred to a white well plate and mixed with 1mM luciferin salt (Anaspec) diluted in 0.1M potassium phosphate buffer containing 0.1M magnesium sulfate. The luminescence was measured using a Wallace 1450 Microbeta luminescence reader at a wavelength of 490 nM.

Synergy Analysis

For synergy analysis, the cell infection inhibition assay was set up as described above with LJC-240-L4, UM15, chimera **11** and the combination of LJC-240-L4 and UM15 at 1:30 ratio based on the initially derived IC_{50} values. Values of percent Bal.01 infection were plotted against the concentration of each inhibitor used in the combination, and the IC_{50} values were calculated and compared with the IC_{50} values of chimera derived from the same experiment. The IC_{50} values so determined were plotted in an isobologram to assess the synergistic effect of both noncovalent mixture and chimera.

HIV specificity and cytotoxicity

HIV specificity was observed by performing an infection inhibition analysis of the bifunctional chimera against Amyotrophic leukemia virus (AMLV) along with pseudotyped

HIV-1. In addition, infection inhibition activities were evaluated with the functionally CD4-independent virus mutant J1HX N197S and compared to the non-mutated and CD-4 dependent parent virus (J1HX)[32]. Briefly, viruses were treated for 30 minutes at 37 °C with inhibitor and then added to HOS cells. The infection was carried out for 24 hours before a media change was performed to remove any residual virus or inhibitor. Production of reporter luciferase was allowed to continue for an additional 24 hours before lysing the cells with passive lysis buffer (Promega) and performing a luciferase assay to quantify the signal.

Cytotoxicity of the bifunctional chimera **11** was measured by performing a colorimetric assay designed to measure the relative proliferation rates of cells in culture. Briefly the cells were treated with serially diluted bifunctional chimera for 24 hours, after which a tetrazolium salt WST-1 was added to the cells. Viability of cells was measured by detecting the conversion of the tetrazolium salt WST-1 into a colored dye (Optical density measurement at 400 nM) by mitochondrial dehydrogenase enzymes functional only in live cells.

Shedding Protocol

HIV-1 shedding was determined by performing a western blot analysis to observe the amount of shed gp120 when viruses were treated with the bifunctional chimera **11** and UM15. Pseudovirus BaL.01 were produced and purified as described above. Ninety (90) □L aliquots of purified BaL.01 pseudovirus were mixed with 10 □L compounds (UM15 or LJC240-L4-UM15) at various dilutions or PBS (served as negative control). The mixtures were incubated for 18 h at 37 °C, followed by a spin at 15,000 rpm at 4°C for 2 h. Eighty (80) □L supernatant from the mixtures were taken and separated by 10% SDS-PAGE gel electrophoresis. Then western blot was used to determine the gp120 content in the

supernatant with primary anti-gp120 antibody, D7324, and secondary antibody, anti-sheep HRP. ImageJ was used to determine Western blot band densities.

Surface Plasmon Resonance Interaction Analysis

SPR experiments were performed on a BIACORE 3000 optical biosensor (GE) at 25 °C using standard PBS buffer containing 0.005% tween 20 and 2% DMSO. Three flow cells in a CM5 chip were used for amine coupling of different ligands using standard 1-ethyl-3-(3-(dimethylamino)propyl) carbodiimide (EDC)/N-hydroxysuccinamide (NHS) chemistry. Flow cell 1 containing ~ 2000 RUs of immobilized 2B6R antibody served as a control for flow cells 2 and 3 containing 2000 RUs of CD4 and 17b antibody respectively. 200 nM of gp120 in the presence of increasing concentrations of LJC240-L4-UM15 (**11**) and UM15 were injected over flow cells 1, 2 and 3. After each sample run, bound gp120 was removed with 10mM HCl (2 pulses of 10s). All experiments were done in sets of three. Data analysis was performed using BIAevaluation V4.1.1 software (GE). To correct for nonspecific binding, response signals from buffer injection and from control flow cell were subtracted from all sensograms. Inhibition data were determined by calculating the inhibitor concentration required for 50% inhibition of maximal binding (IC_{50}). The inhibition curve was plotted and then fitted using the four-parameter equation (1) as shown below using Origin Pro 8 graphing software.

$$Equation\ (1)\ Response = Rhigh - \frac{Rhigh - Rlow}{1 + \left(\frac{concn}{A1}\right) A2}$$

where, R_{high} is the response at the highest inhibitor concentration and R_{low} at low inhibitor concentration, concn is the concentration of inhibitor and A1 and A2 are fitting parameters.

Calcium Mobilization Assay

CHO cells stably expressing CCR5 and Gα16 were loaded with 2 μmol/L Fluo-4 AM in Hanks balanced salt solution (HBSS, containing KCl 5.4 mM, Na_2HPO_4 0.3 mM, KH_2PO_4 0.4 mM, $NaHCO_3$ 4.2 mM, $CaCl_2$ 1.3 mM, $MgCl_2$ 0.5 mM, Mg_2SO_4 0.6 mM, NaCl 137 mM, BSA 5 g/L, Glucose 5.6 mM, Sulfinpyrazone 250 μM, pH 7.4) at 37 °C for 45 minutes. After the cells being rinsed with the reaction buffer, HBSS (50 μL) containing known antagonists as a positive control, compounds of interest or DMSO (negative control, final concentration 1%) were added. After incubation at room temperature for 10 minutes, RANTES (25 μL; final concentration 30 nM) was dispensed into the well using a FlexStation II micro-plate reader (Molecular Devices, Sunnyvale, CA, USA) and intracellular calcium change was recorded with an excitation wavelength of 485 nm and emission wavelength of 525 nm. The half maximal inhibitory concentrations (IC_{50}) of compounds were determined with GraphPad Prism software by constructing their dose-response curves.

Cellular Chemotaxis Assay

CEM CCR5 cells were re-suspended to a density of 2.0×10^6/ml in RPMI-1640 medium containing 0.1% BSA and 10% FBS. Cells were pre-incubated with Maraviroc, LJC240, LJC240-L4, and LJC240-L4-UM15 (**11**) at the IC_{50} values indicated in **Figure 9** for 15 minutes at room temperature. 1.0×10^6 cells (500 μl) were seeded in smooth-walled inserts containing polycarbonate membranes with 8 μm pores in a 24-well tissue culture plate (BrandTech, Essex, CT). 1 ml of complete medium containing RANTES (10 ng/ml) was added to the lower chamber, and plates were incubated for 6 hours at 37 °C in 5% CO_2. Complete media only served as a control for RANTES-induced migration. Migrated cells that adhered to the basolateral surface of the insert were dissociated by incubating inserts in 1 ml HBSS with 1 mM EDTA for 30 minutes at 37 °C in 5% CO_2. 10 μl of a 1:1 mixture of cells from the basolateral chamber and dissociated cells was then mixed with 10

µl of trypan blue and live cells were counted using the Countess automated cell counter (Thermo Scientific, Waltham, MA). Two-way ANOVA was used to compare the inhibitor treated groups to the RANTES only control group and Student's T- test was used to compare individual groups. Error bars represent mean ± SEM. *=p≤ 0.05, **p ≤0.01.

COMPETING FINANCIAL INTERESTS

The authors declare no competing financial interests.

AUTHOR INFORMATION

* Corresponding authors: Y.-Q. Long, Tel: +86-512-65882275, email: longyaqiu@suda.edu.cn; I. Chaiken, Tel: +1-215-762-4197, email: imc23@drexel.edu)

Funding: National Natural Science Foundation of China to YQL (81761128022, 81361120410, 81325020) and National Institutes of Health to IC (R01AI106633, P01GM56550).

AUTHOR CONTRIBUTIONS

AAR, APH, YQL, and IC wrote the main manuscript text. AAR designed, synthesized and purified the LJC240-L4-UM15 bifunctional chimera, and managed the experimental path of the chimera evaluation. AAR and LS designed and synthesized component inhibitors. APH and KA designed and performed the virological studies that demonstrated infection inhibition functions and synergistic activities. KA performed the SPR experiments. SZ performed the gp120 shedding assays. ZLW and XX performed the calcium mobilization assays. EG and MAK performed the chemotaxis assays. VP helped with the synergy analysis. YQL and IC jointly directed the project. All authors reviewed the manuscript.

AKNOWLEDGEMENT

We thank Openeye Scientific Software (Santa Fe, NM. http://www.eyesopen.com) for providing a complimentary academic license of their software package.

ABBREVIATIONS USED

ACN, acetonitrile; Boc, Tertbutyloxycarbonyl; DIC, N,N′-Diisopropylcarbodiimide; DMF, Dimethylformamide; Env, HIV envelope gp160; Fmoc, 9-Fluorenylmethoxycarbonyl; HPLC, high performance liquid chromatography; HOBT, Hydroxybenzotriazole; PT, Peptide triazole; SPR, Surface Plasmon Resonance; tBu, Tert-butyl; TIPS, Triisoproylsilane; Trt, Triphenylmethyl; TFA, Trifluoroacetic acid; wt, wild type.

SUPPORTING INFORMATION

PDB files of the docked inhibitors and molecular formula strings are available

REFERENCES

1. Wilen, C. B.; Tilton, J. C.; Doms, R. W. Hiv: Cell binding and entry. *Cold Spring Harb Perspect Med* **2012,** *2*.
2. Dorr, P.; Westby, M.; Dobbs, S.; Griffin, P.; Irvine, B.; Macartney, M.; Mori, J.; Rickett, G.; Smith-Burchnell, C.; Napier, C.; Webster, R.; Armour, D.; Price, D.; Stammen, B.; Wood, A.; Perros, M. Maraviroc (uk-427,857), a potent, orally bioavailable, and selective small-molecule inhibitor of chemokine receptor CCR5 with broad-spectrum anti-human immunodeficiency virus type 1 activity. *Antimicrob Agents Chemother* **2005,** *49*, 4721-4732.
3. Lieberman-Blum, S. S.; Fung, H. B.; Bandres, J. C. Maraviroc: A CCR5-receptor antagonist for the treatment of hiv-1 infection. *Clin Ther* **2008,** *30*, 1228-1250.
4. Este, J. A.; Telenti, A. Hiv entry inhibitors. *Lancet* **2007,** *370*, 81-88.

5. Yost, R.; Pasquale, T. R.; Sahloff, E. G. Maraviroc: A coreceptor CCR5 antagonist for management of hiv infection. *Am J Health Syst Pharm* **2009,** *66*, 715-726.

6. Greenberg, M. L.; Cammack, N. Resistance to enfuvirtide, the first hiv fusion inhibitor. *J Antimicrob Chemother* **2004,** *54*, 333-340.

7. Eggink, D.; de Taeye, S. W.; Bontjer, I.; Klasse, P. J.; Langedijk, J. P.; Berkhout, B.; Sanders, R. W. Hiv-1 escape from a peptidic anchor inhibitor through stabilization of the envelope glycoprotein spike. *J Virol* **2016,** *90*, 10587-10599.

8. Nakata, H.; Steinberg, S. M.; Koh, Y.; Maeda, K.; Takaoka, Y.; Tamamura, H.; Fujii, N.; Mitsuya, H. Potent synergistic anti-human immunodeficiency virus (hiv) effects using combinations of the CCR5 inhibitor aplaviroc with other anti-hiv drugs. *Antimicrob Agents Chemother* **2008,** *52*, 2111-2119.

9. Tremblay, C. L.; Giguel, F.; Guan, Y.; Chou, T. C.; Takashima, K.; Hirsch, M. S. Tak-220, a novel small-molecule CCR5 antagonist, has favorable anti-human immunodeficiency virus interactions with other antiretrovirals in vitro. *Antimicrob Agents Chemother* **2005,** *49*, 3483-3485.

10. Tremblay, C. L.; Giguel, F.; Kollmann, C.; Guan, Y.; Chou, T. C.; Baroudy, B. M.; Hirsch, M. S. Anti-human immunodeficiency virus interactions of sch-c (sch 351125), a CCR5 antagonist, with other antiretroviral agents in vitro. *Antimicrob Agents Chemother* **2002,** *46*, 1336-1339.

11. Tremblay, C. L.; Kollmann, C.; Giguel, F.; Chou, T. C.; Hirsch, M. S. Strong in vitro synergy between the fusion inhibitor t-20 and the CXCR4 blocker amd-3100. *J Acquir Immune Defic Syndr* **2000,** *25*, 99-102.

12. Doms, R. W.; Peiper, S. C. Unwelcomed guests with master keys: How hiv uses chemokine receptors for cellular entry. *Virology* **1997,** *235*, 179-190.

13. Fan, X.; Zhang, H. S.; Chen, L.; Long, Y. Q. Efficient synthesis and identification of novel propane-1,3-diamino bridged CCR5 antagonists with variation on the basic center carrier. *Eur J Med Chem* **2010,** *45*, 2827-2840.

14. Feng, D. Z.; Song, Y. L.; Jiang, X. H.; Chen, L.; Long, Y. Q. Forward- and reverse-synthesis of piperazinopiperidine amide analogs: A general access to structurally diverse 4-piperazinopiperidine-based CCR5 antagonists. *Org Biomol Chem* **2007,** *5*, 2690-2697.

15. Long, Y. Q.; Feng, D. Z.; Chen, L.; Chen, R. H. 1-(3-Amino-Propyl)-Piperidin-4-yl-Amides, Pharmaceutical Compositions, Processes For Their Preparation And Uses. WO2009052708A1. April 30, 2009.

16. Zhang, H. S.; Feng, D. Z.; Chen, L.; Long, Y. Q. Discovery of novel (s)-alpha-phenyl-gamma-amino butanamide containing CCR5 antagonists via functionality inversion approach. *Bioorg Med Chem Lett* **2010,** *20*, 2219-2223.

17. Cao, B. L., Y.; Wei, W.; Xie, X. New Imidazopyridine Compound Useful In Pharmaceutical Composition and In Preparation Of Medicine For Treating Dieseases From Hiv Virus Infection, Rheumatoid Arthritis, Inflammation, and Cancer. CN 102675305 B. March 08, 2011.

18. Bastian, A. R.; Kantharaju; McFadden, K.; Duffy, C.; Rajagopal, S.; Contarino, M. R.; Papazoglou, E.; Chaiken, I. Cell-free hiv-1 virucidal action by modified peptide triazole inhibitors of env gp120. *ChemMedChem* **2011,** *6*, 1335-1339.

19. Rashad, A. A.; Kalyana Sundaram, R. V.; Aneja, R.; Duffy, C.; Chaiken, I. Macrocyclic envelope glycoprotein antagonists that irreversibly inactivate hiv-1 before host cell encounter. *J Med Chem* **2015,** *58*, 7603-7608.

20. Aneja, R.; Rashad, A. A.; Li, H.; Kalyana Sundaram, R. V.; Duffy, C.; Bailey, L. D.; Chaiken, I. Peptide triazole inactivators of hiv-1 utilize a conserved two-cavity binding

site at the junction of the inner and outer domains of env gp120. *J Med Chem* **2015,** *58*, 3843-3858.

21. Gopi, H.; Umashankara, M.; Pirrone, V.; LaLonde, J.; Madani, N.; Tuzer, F.; Baxter, S.; Zentner, I.; Cocklin, S.; Jawanda, N.; Miller, S. R.; Schon, A.; Klein, J. C.; Freire, E.; Krebs, F. C.; Smith, A. B.; Sodroski, J.; Chaiken, I. Structural determinants for affinity enhancement of a dual antagonist peptide entry inhibitor of human immunodeficiency virus type-1. *J Med Chem* **2008,** *51*, 2638-2647.
22. Gopi, H. N.; Tirupula, K. C.; Baxter, S.; Ajith, S.; Chaiken, I. M. Click chemistry on azidoproline: High-affinity dual antagonist for hiv-1 envelope glycoprotein gp120. *ChemMedChem* **2006,** *1*, 54-57.
23. Kamanna, K.; Aneja, R.; Duffy, C.; Kubinski, P.; Rodrigo Moreira, D.; Bailey, L. D.; McFadden, K.; Schon, A.; Holmes, A.; Tuzer, F.; Contarino, M.; Freire, E.; Chaiken, I. M. Non-natural peptide triazole antagonists of hiv-1 envelope gp120. *ChemMedChem* **2013,** *8*, 322-328.
24. Umashankara, M.; McFadden, K.; Zentner, I.; Schon, A.; Rajagopal, S.; Tuzer, F.; Kuriakose, S. A.; Contarino, M.; Lalonde, J.; Freire, E.; Chaiken, I. The active core in a triazole peptide dual-site antagonist of hiv-1 gp120. *ChemMedChem* **2010,** *5*, 1871-1879.
25. Julien, J. P.; Cupo, A.; Sok, D.; Stanfield, R. L.; Lyumkis, D.; Deller, M. C.; Klasse, P. J.; Burton, D. R.; Sanders, R. W.; Moore, J. P.; Ward, A. B.; Wilson, I. A. Crystal structure of a soluble cleaved hiv-1 envelope trimer. *Science* **2013,** *342*, 1477-1483.
26. Tan, Q.; Zhu, Y.; Li, J.; Chen, Z.; Han, G. W.; Kufareva, I.; Li, T.; Ma, L.; Fenalti, G.; Li, J.; Zhang, W.; Xie, X.; Yang, H.; Jiang, H.; Cherezov, V.; Liu, H.; Stevens, R. C.; Zhao, Q.; Wu, B. Structure of the CCR5 chemokine receptor-hiv entry inhibitor maraviroc complex. *Science* **2013,** *341*, 1387-1390.

27. Huang, C. C.; Lam, S. N.; Acharya, P.; Tang, M.; Xiang, S. H.; Hussan, S. S.; Stanfield, R. L.; Robinson, J.; Sodroski, J.; Wilson, I. A.; Wyatt, R.; Bewley, C. A.; Kwong, P. D. Structures of the CCR5 n terminus and of a tyrosine-sulfated antibody with hiv-1 gp120 and CD4. *Science* **2007,** *317*, 1930-1934.

28. Lee, J. H.; Ozorowski, G.; Ward, A. B. Cryo-em structure of a native, fully glycosylated, cleaved hiv-1 envelope trimer. *Science* **2016,** *351*, 1043-1048.

29. Tallarida, R. J. An overview of drug combination analysis with isobolograms. *J Pharmacol Exp Ther* **2006,** *319*, 1-7.

30. Emileh, A.; Tuzer, F.; Yeh, H.; Umashankara, M.; Moreira, D. R.; Lalonde, J. M.; Bewley, C. A.; Abrams, C. F.; Chaiken, I. M. A model of peptide triazole entry inhibitor binding to hiv-1 gp120 and the mechanism of bridging sheet disruption. *Biochemistry* **2013,** *52*, 2245-2261.

31. Tuzer, F.; Madani, N.; Kamanna, K.; Zentner, I.; LaLonde, J.; Holmes, A.; Upton, E.; Rajagopal, S.; McFadden, K.; Contarino, M.; Sodroski, J.; Chaiken, I. Hiv-1 env gp120 structural determinants for peptide triazole dual receptor site antagonism. *Proteins* **2013,** *81*, 271-290.

32. Kolchinsky, P.; Kiprilov, E.; Bartley, P.; Rubinstein, R.; Sodroski, J. Loss of a single n-linked glycan allows CD4-independent human immunodeficiency virus type 1 infection by altering the position of the gp120 v1/v2 variable loops. *J Virol* **2001,** *75*, 3435-3443.

33. Pancera, M.; Zhou, T.; Druz, A.; Georgiev, I. S.; Soto, C.; Gorman, J.; Huang, J.; Acharya, P.; Chuang, G. Y.; Ofek, G.; Stewart-Jones, G. B.; Stuckey, J.; Bailer, R. T.; Joyce, M. G.; Louder, M. K.; Tumba, N.; Yang, Y.; Zhang, B.; Cohen, M. S.; Haynes, B. F.; Mascola, J. R.; Morris, L.; Munro, J. B.; Blanchard, S. C.; Mothes, W.; Connors, M.; Kwong, P. D. Structure and immune recognition of trimeric pre-fusion hiv-1 env. *Nature* **2014,** *514*, 455-461.

34. Borsi, V.; Calderone, V.; Fragai, M.; Luchinat, C.; Sarti, N. Entropic contribution to the linking coefficient in fragment based drug design: A case study. *J Med Chem* **2010,** *53*, 4285-4289.

35. Ji, C.; Kopetzki, E.; Jekle, A.; Stubenrauch, K. G.; Liu, X.; Zhang, J.; Rao, E.; Schlothauer, T.; Fischer, S.; Cammack, N.; Heilek, G.; Ries, S.; Sankuratri, S. CD4-anchoring hiv-1 fusion inhibitor with enhanced potency and in vivo stability. *J Biol Chem* **2009,** *284*, 5175-5185.

36. Kagiampakis, I.; Gharibi, A.; Mankowski, M. K.; Snyder, B. A.; Ptak, R. G.; Alatas, K.; LiWang, P. J. Potent strategy to inhibit hiv-1 by binding both gp120 and gp41. *Antimicrob Agents Chemother* **2011,** *55*, 264-275.

37. Kopetzki, E.; Jekle, A.; Ji, C.; Rao, E.; Zhang, J.; Fischer, S.; Cammack, N.; Sankuratri, S.; Heilek, G. Closing two doors of viral entry: Intramolecular combination of a coreceptor- and fusion inhibitor of hiv-1. *Virol J* **2008,** *5*, 56.

38. Parajuli, B.; Acharya, K.; Yu, R.; Ngo, B.; Rashad, A. A.; Abrams, C. F.; Chaiken, I. M. Lytic inactivation of human immunodeficiency virus by dual engagement of gp120 and gp41 domains in the virus env protein trimer. *Biochemistry* **2016,** *55*, 6100-6114.

39. Quinlan, B. D.; Joshi, V. R.; Gardner, M. R.; Ebrahimi, K. H.; Farzan, M. A double-mimetic peptide efficiently neutralizes hiv-1 by bridging the CD4- and coreceptor-binding sites of gp120. *J Virol* **2014,** *88*, 3353-3358.

40. Zhao, B.; Mankowski, M. K.; Snyder, B. A.; Ptak, R. G.; Liwang, P. J. Highly potent chimeric inhibitors targeting two steps of hiv cell entry. *J Biol Chem* **2011,** *286*, 28370-28381.

41. Martinez-Munoz, L.; Barroso, R.; Dyrhaug, S. Y.; Navarro, G.; Lucas, P.; Soriano, S. F.; Vega, B.; Costas, C.; Munoz-Fernandez, M. A.; Santiago, C.; Rodriguez Frade, J.

M.; Franco, R.; Mellado, M. CCR5/CD4/CXCR4 oligomerization prevents hiv-1 gp120iiib binding to the cell surface. *Proc Natl Acad Sci U S A* **2014,** *111*, E1960-1969.

42. Jiang, X.; Feyertag, F.; Meehan, C. J.; McCormack, G. P.; Travers, S. A.; Craig, C.; Westby, M.; Lewis, M.; Robertson, D. L. Characterizing the diverse mutational pathways associated with r5-tropic maraviroc resistance: Hiv-1 that uses the drug-bound CCR5 coreceptor. *J Virol* **2015,** *89*, 11457-11472.

43. Rashad, A. A.; Acharya, K.; Haftl, A.; Aneja, R.; Dick, A.; Holmes, A. P.; Chaiken, I. Chemical optimization of macrocyclic hiv-1 inactivators for improving potency and increasing the structural diversity at the triazole ring. *Org Biomol Chem* **2017,** *15*, 7770-7782.

44. De Clercq, E. The bicyclam amd3100 story. *Nat Rev Drug Discov* **2003,** *2*, 581-587.

45. Long, Y. Q. C., B.; Xi, X.; Wei, W. Imidazopyridines as CXCR4 Antagonists and Their Preparation, Pharmaceutical Compositions and Use In The Treatment Of Diseases. CN 102675305, September 19, 2012.

46. Sastry, G. M.; Adzhigirey, M.; Day, T.; Annabhimoju, R.; Sherman, W. Protein and ligand preparation: Parameters, protocols, and influence on virtual screening enrichments. *J Comput Aided Mol Des* **2013,** *27*, 221-234.

47. Acharya, K.; Rashad, A. A.; Moraca, F.; Klasse, P. J.; Moore, J. P.; Abrams, C.; Chaiken, I. Recognition of hiv-inactivating peptide triazoles by the recombinant soluble env trimer, bg505 sosip.664. *Proteins* **2017**, *85*, 843-851.

48. Murphy, R. R., M.; Zhou, Z. Y.; Abel, R.; Krilov, G.; Tubert-Brohman, I.; Sherman, W.; Farid, R.; Friesner, R. A. Evaluation of docking and scoring accuracy using a new version of schrodinger's glide xp and induced fit docking (ifd) methodologies. *Abstr. Pap. Am. Chem. Soc.* **2011**, *241*, 93.

49. Zhao, G. L.; Lin, S.; Korotvička, A.; Deiana, L.; Kullberg, M.; Córdova, A. Asymmetric synthesis of maraviroc (uk ‐ 427,857). *Advanced Synthesis & Catalysis* **2010,** *352*, 2291-2298.

50. Haycock-Lewandowski, S. J.; Wilder, A.; Åhman, J. Development of a bulk enabling route to maraviroc (uk-427,857), a ccr-5 receptor antagonist. *Organic Process Research & Development* **2008,** *12*, 1094-1103.

51. Asano, S.; Gavrilyuk, J.; Burton, D. R.; Barbas, C. F., 3rd. Preparation and activities of macromolecule conjugates of the CCR5 antagonist maraviroc. *ACS Med Chem Lett* **2014,** *5*, 133-137.

52. Kiely, J. S.; Hutt, M. P.; Culbertson, T. P.; Bucsh, R. A.; Worth, D. F.; Lesheski, L. E.; Gogliotti, R. D.; Sesnie, J. C.; Solomon, M.; Mich, T. F. Quinolone antibacterials: Preparation and activity of bridged bicyclic analogues of the c7-piperazine. *J Med Chem* **1991,** *34*, 656-663.

53. Hu, S.; Wang, Z.; Hou, T.; Ma, X.; Li, J.; Liu, T.; Xie, X.; Hu, Y. Design, synthesis, and biological evaluation of novel 2-methylpiperazine derivatives as potent CCR5 antagonists. *Bioorganic & Medicinal Chemistry* **2015,** *23*, 1157-1168.

54. Bastian, A. R.; Contarino, M.; Bailey, L. D.; Aneja, R.; Moreira, D. R.; Freedman, K.; McFadden, K.; Duffy, C.; Emileh, A.; Leslie, G.; Jacobson, J. M.; Hoxie, J. A.; Chaiken, I. Interactions of peptide triazole thiols with env gp120 induce irreversible breakdown and inactivation of hiv-1 virions. *Retrovirology* **2013,** *10*, 153.

55. McFadden, K.; Fletcher, P.; Rossi, F.; Kantharaju; Umashankara, M.; Pirrone, V.; Rajagopal, S.; Gopi, H.; Krebs, F. C.; Martin-Garcia, J.; Shattock, R. J.; Chaiken, I. Antiviral breadth and combination potential of peptide triazole hiv-1 entry inhibitors. *Antimicrob Agents Chemother* **2012,** *56*, 1073-1080.

Table Of Contents Graphic